Desalination and Water Treatment
www.deswater.com
doi: 10.1080/19443994.2013.873994

53 (2015) 3615–3622
March

Taylor & Francis
Taylor & Francis Group

Removal of Disperse Orange 25 using *in situ* surface-modified iron-doped TiO_2 nanoparticles

B. Shahmoradi[a,*], A. Maleki[a], K. Byrappa[b]

[a]*Kurdistan Environmental Health Research Center, Kurdistan University of Medical Sciences, Sanandaj, Iran*
Tel. +98 918 770 5355, Fax: +98 871 662 5131; email: bshahmorady@gmail.com
[b]*Department of Earth Science, University of Mysore, Manasagangothri, Mysore, India*

Received 25 June 2013; Accepted 4 December 2013

ABSTRACT

Disperse Orange 25 (DO25) is one of the strong azo dyes, which makes its degradation too difficult. Photodegradation of this dye was conducted using in situ surface modified iron doped TiO_2 nanoparticles under sunlight. The nanoparticles were synthesized under mild hydrothermal conditions (p = autogeneous, $T = 100\,^{\circ}C$, $t = 18$ h) using Fe_2O_3 and n-butyleamine as dopant and surface modifier respectively. The nanoparticles synthesized were characterized systematically using powder XRD, FTIR, SEM, EDAX, BET surface area, BJT, porosity, and UV–vis spectroscopy. The photodegradation variables were dye concentration, photocatalyst load, time duration, and pH. The removal efficiency was determined using UV–vis spectrophotometer and TOC analyzer. The results revealed that *in situ* surface modified iron doped TiO_2 nanoparticles could remarkably degrade high concentration of DO25 under sunlight, which could not be achieved for reagent grade TiO_2.

Keywords: Disperse Orange 25; Fe doped TiO_2 nanoparticles; Surface modification; Hydrothermal conditions

1. Introduction

Textile dyes and other industrial dyestuffs have constituted one of the largest and most versatile organic groups intimidating the environment [1]. Dyes are widely used in different industries and their discharge into water bodies without or with partial treatment brings about not only unattractive water and aesthetic problems but also reduces the autopurification capacity of the receiving waters; therefore, water pollution and ecological problems occur [2,3]. Due to the stability of modern dyes, conventional biological treatments cannot degrade the dyes completely and the sludge produced requires post treatment; hence, they are not cost-effective.

Heterogeneous photocatalysis is a promising technique which can be successfully used to eliminate toxic and bioresistant pollutants, including azo dyes from aqueous solutions, through transformation into benign compounds [4]. In this regard, TiO_2 is the most widely used photocatalyst due to its non-toxicity, high activity, large stability, and cost-effectiveness [5]. To achieve effective decomposition of organic compounds, design and development of photocatalysts

*Corresponding author.

with high levels of activities are needed [6]. The vital snag of TiO_2 semiconductor is that it absorbs a small portion of solar spectrum in the UV region (at $\lambda \leq 400$ nm) [7]. Under UV light illumination, TiO_2 undergoes charge transfer processes and produces electron-hole pairs on the surface [8]. Hence, in order to harvest maximum solar energy, it is necessary to shift the absorption threshold towards visible light. Doping is a promising strategy to shift the absorption threshold towards visible lights. There are several reports on doping TiO_2 with molybdenum, tungsten, neodymium, and other metal oxides [9–11], or other compounds. Another problem with nanoparticles is their agglomeration and less dispersion in medium.

There are various methods of synthesizing nanoparticles including sol–gel [12], CVD [13], chemical precipitation [14], anodic oxidation [15], and hydrothermal technique. Mild hydrothermal technique is an eco-friendly and a cost-effective method in which control over morphology and agglomeration can be achieved.

Thus, to overcome the above-mentioned drawbacks, iron-doped TiO_2 nanoparticles were synthesized using Fe_2O_3 as dopant and *n*-butyleamine as surface modifier under mild hydrothermal conditions and their photodegradation efficiency was evaluated through photodegradation of Disperse Orange 25 (DO25) at different conditions.

2. Materials and methods

2.1. Fabrication of in situ surface-modified Fe:TiO_2 nanoparticles

Iron-doped TiO_2 (Fe:TiO_2) nanoparticles were synthesized under mild hydrothermal conditions ($T = 100$ °C, p = autogeneous, $t = 16$ h) [9,10]. Fe:TiO_2 nanoparticles were synthesized under four different conditions by varying the dopant percentage and amount of surface modifier. We labeled the resultant samples as Fe:TiO_2I, Fe:TiO_2II, Fe:TiO_2III, and Fe:TiO_2IV, respectively. In brief, we took 1 mol of pure TiO_2 (Merck, AG, 99%) as starting material and the dopant, Fe_2O_3 (Merck, AG, 99%), at 1 and 2 M % was added into it and it was stirred vigorously for a few minutes. The final compound was then transferred to a 25 mL Teflon liner (Vfill = 50%), which was later placed inside a General-Purpose autoclave. The assembled autoclave was kept in an oven with a temperature programmer/controller for 16 h. The temperature was kept at 100 °C. After the experimental run, the autoclave was cooled to room temperature. The product in the Teflon liner was then transferred to a clean beaker, washed with double-distilled water (EC < 1 μΩ), and later allowed to settle down. The surplus solution was removed using a syringe and the remnants were centrifuged for 10 min at 4,500 rpm. The product was recovered and dried in a hot air oven at 40–50 °C for a few hours.

2.2. Photocatalytic degradation experiments

Photodegradation of DO25 (Alvand Sabet, Iran) in aqueous media was tested using the nanoparticles synthesized. Different dye concentrations (20, 40, 60, 80, and 100 mg/L) were prepared using stock solution. The reaction suspension was prepared by adding different amounts (0.4–1.0 g) of photocatalyst powder per a liter of dye solution. Prior to irradiation, the reaction mixture was kept in darkness for 30 min under continuous shaking to ensure balance adsorption–desorption equilibrium. The mixture was then irradiated with sunlight. All of the experiments were carried out from 11:30 a.m. to 2:00 p.m. (July 2012). In order to utilize sunlight more efficiently, the outdoor experiments were carried out with 250 mL Pyrex glass reservoirs placed on shakers exposed to direct sunlight on the roof of the laboratory building. The ambient temperature while carrying out the experiments was about 38 ± 3 °C. All the Pyrex glass beakers containing dye samples and nanoparticles were covered with a very thin cellophane transparent cover. For comparison purpose, a blank experiment was carried out along with other experiments. The suspensions were sampled at specific intervals (30, 60, 90, and 120 min) to monitor the changes in DO25 concentration. No external aeration was applied to make the method more cost-effective. Suspensions sampled were centrifuged at 4,500 rpm for 30 min to remove the *in situ* surface-modified Fe:TiO_2 nanoparticles and then analyzed using a double-beam UV–vis spectrophotometer at 425 nm (λ_{max}) corresponding to the maximal absorption of the dye. TOC was measured using TOC Analyzer (Skalar, the Netherlands) according to standard methods [16].

3. Results and discussion

The powder XRD data reveal a highly crystallized anatase structure, matched well with the *I*4/*amd* space group and there was no new peak, which confirms that iron has been doped to TiO_2 without changing the structure (Fig. 1). The slight change in the lattice parameters of the Fe:TiO_2 nanoparticles confirms the existence of iron atoms in TiO_2 nanoparticles. As Fig. 1 indicates, all of the powder XRD patterns of the nanoparticles are quite similar. The radii of the Fe ions

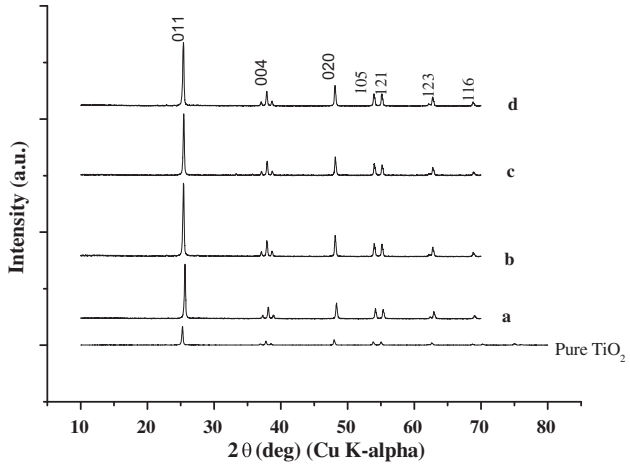

Fig. 1. Powder XRD of surface-modified iron-doped TiO_2 nanoparticles. (a) 1 mol % dopant, 0.5 mL surface modifier; (b) 1 mol %, 1 mL; (c) 2 mol %, 0.5 mL; and (d) 2 mol % dopant, 1 mL surface modifier.

Table 1
Cell parameters of *in situ* surface-modified Fe:TiO_2 nanoparticles

Catalyst	*a* (Å)	*c* (Å)	*a*:*c* ratio	*V* (Å^3)	References
RG TiO_2	3.7845	9.5143	0.3977	136.27	[17]
Fe: TiO_2 I	3.7718	9.4736	0.3981	134.78	PW
Fe:TiO_2 II	3.7846	9.5065	0.3981	136.22	PW
Fe:TiO_2 III	3.7826	9.5005	0.3981	135.94	PW
Fe:TiO_2 IV	3.7838	9.5109	0.3978	136.17	PW

RG = Reagent grade; I = 1 mol % dopant, 0.5 mL surface modifier; II = 1 mol % dopant, 1.0 mL surface modifier; III =2 mol % dopant, 0.5 mL surface modifier; and IV = 2 mol % dopant, 1.0 mL surface modifier. PW = Present work.

(49 pm) are bigger than those of the Ti (42 pm); therefore, doping Fe (VI) should make the cell volume bigger than reagent grade TiO_2. However, it was found that doping with Fe_2O_3 reduced the cell parameters of TiO_2 as determined using Chekcell software (Table 1). This reduction in cell parameters and cell volume may be attributed to the effect of the surface modifier on crystal growth and its morphology. As Table 1 indicates, the cell volume of iron (1 mol %) doped TiO_2 nanoparticles, modified using 0.5 mL surface modifier, was significantly smaller (0.13478 nm^3) compared with other nanoparticles synthesized. The powder XRD pattern of (1 mol %; 2 mol %) *in situ* surface-modified Fe:TiO_2 nanoparticles shows seven primary peaks, which can be attributed to different diffraction planes of TiO_2 [18]. Moreover, the powder XRD patterns revealed that the intensity of the peaks for iron (1 mol %) doped TiO_2 nanoparticles modified using 0.5 mL *n*-butylamine was the highest. This fact has been overlooked due to overlaying of XRD graphs in Fig. 1.

The crystallite size of the products was determined from the line broadening of the peak (101) using Scherrer's equation [19]. Table 2 lists some of the required characteristics of the samples synthesized, such as crystallite size, BET surface area, micropore area, micropore volume, average pore diameter, element content, and cell volume parameters.

Total pore volumes were estimated from nitrogen adsorption at a pressure of 101.12 kPa. BET measurements confirmed the absence of macropores in all nanoparticles. Although the BET surface area was very less, the pore surface area was less than BET surface area, which in general indicates high surface area of the nanoparticles synthesized.

Table 3 shows the FTIR data for iron-doped TiO_2 nanoparticles. We used KBr method for FTIR analysis in which KBr is used as background sample. The peaks' intensity of reagent grade was too weak compared with surface-modified Fe:TiO_2 nanoparticles, so that it was not overlaid with other samples. On the other hand, the peaks' intensity of 2 mol % Fe:TiO_2 nanoparticles modified using 1.0 mL *n*-butylamine was extremely high; hence, it was excluded from the FTIR spectra (Fig. 2). The same phenomena happened in the case of reagent grade TiO_2. Therefore, the characteristic peaks of 1 mol % Fe:TiO_2 nanoparticles

Table 2
The textural properties of *in situ* surface-modified iron-doped TiO_2 nanoparticles

Catalyst	Crystallite size of nanoparticles	S_{BET} (m^2/g)	a_p (m^2/g)	$R_{p,\ peak}$ (nm)	V_m (cm^3/g)	V_{tot} (cm^3/g)	D_p (nm)	EDX Fe–Ti%
Fe:TiO_2 I	48	9.0112	5.9428	2.41	2.0704	0.0064	28.242	3.24–94.18
Fe:TiO_2 II	39	8.0748	6.4744	2.41	1.8552	0.0059	29.138	3.98–92.26
Fe:TiO_2 III	53	5.0186	3.3583	86.28	1.1675	0.0062	49.027	3.66–92.78
Fe:TiO_2 IV	64	5.9291	5.5500	12.24	1.3622	0.0056	37.778	3.88–93.23

S_{BET}: BET surface area; a_p: pore surface area; V_m: volume of pore, V_{tot}: total volume of pore; and D_p: mean diameter of pore.
I: (1 mol % dopant, 0.5 mL surface modifier); II: (1 mol % dopant, 1.0 mL surface modifier); III: (2 mol % dopant, 0.5 mL surface modifier); and IV: (2 mol % dopant, 1.0 mL surface modifier).

Table 3
The characteristic FTIR spectra data for *in situ* surface-modified Fe:TiO_2 nanoparticles

Bands (cm^{-1})			
Fe:TiO_2 I	Fe:TiO_2 II	Fe:TiO_2 III	Fe:TiO_2 IV
3,851	3,667	3,033	3,851
3,732	3,646	1,636	3,564
3,646	2,352	1,401	2,358
1,644	1,634	542	1,644
1,396	1,506	502	1,401
677	1,396	477	720

Note: I = 1 mol % dopant, 0.5 mL surface modifier; II = 1 mol % dopant, 1.0 mL surface modifier; III = 2 mol % dopant, 0.5 mL surface modifier; and IV = 2 mol % dopant, 1.0 mL surface modifier.

modified using 0.5 mL *n*-butylamine is explained as reference. The peaks observed at 3,851–3,646 cm^{-1} correspond to the stretching mode of C=O, amide N–H, and –OH stretching vibration. The peak at 1,644 cm^{-1} can be attributed to C=C bending and stretching modes, whereas the peak at 1,396 cm^{-1}may be due to strong ammonium ion and CH_3–N = (R1, R2). Finally, the peak at 677 cm^{-1} and other peaks around this range could be attributed to O–Ti–O vibration and symmetric Fe–O–Fe stretching vibration [20]. *n*-butylamine is an organic compound which has no positive effect on photodegradation directly. However, as characterization results confirmed, it controls the crystal growth direction and cell parameter values of nanoparticles. Hence, the desired properties of the nanoparticles synthesized can enhance the photodegradation property.

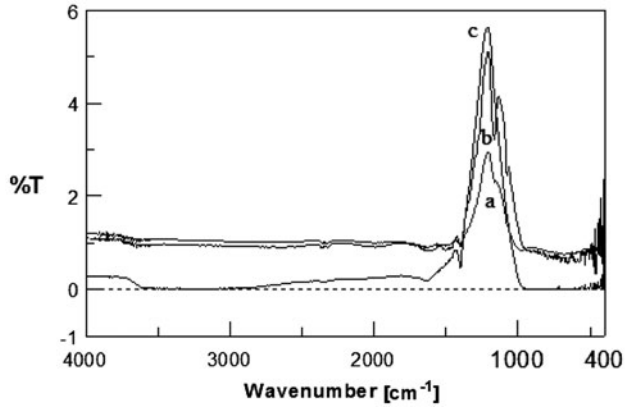

Fig. 2. FTIR spectra of surface-modified iron-doped TiO_2 nanoparticles. (a) 1 mol % dopant, 0.5 mL surface modifier; (b) 1 mol % dopant, 1 mL surface modifier; and (c) 2 mol % dopant, 0.5 mL surface modifier.

Fig. 3 shows the SEM images of *in situ* surface-modified Fe:TiO_2 nanoparticles. The morphologies of the nanoparticles synthesized are quite similar to each other and likely become spherical in general. However, the shape of 2 mol % Fe:TiO_2 nanoparticles modified with 1.0 mL *n*-butylamine is rather different. Although the size distribution of the nanoparticles was not determined, the size of the particles varies in the range of 50–100 nm, as measured using SEM images and Scherrer's equation.

4. Photodegradation of DO25

A series of experiments were executed under different experimental conditions in which the deduction of sunlight absorbance was estimated in order to study the key factors affecting the photodegradation of DO25. Table 4 presents the characteristics of DO25. In all cases, the photodegradation efficiency, i.e. dye removal, was calculated using Eq. (1):

$$\eta = (C_i - C_f)/C_i \times 100 \quad (1)$$

where η = dye removal efficiency, C_i = initial concentration of DO25, and C_f = final concentration of DO25.

4.1. Effect of nanoparticles loading on photodegradation of DO25

In slurry photocatalytic process, catalyst dosage is an important parameter. In order to assess the optimum nanoparticles loading for effective dye degradation, varying amounts (0.4–1.0 g/L) of nanoparticles were attempted. Fig. 4 demonstrates that photodegradation percentage increases with modified Fe:TiO_2 nanoparticles loading. However, the efficiency was almost zero when reagent grade TiO_2 was used; this confirms the effect of doping on photodegradation of DO25. Since it is known that above a certain loading, increase in turbidity of the solution inhibits photodegradation, and hence reduces the light transmission through the solution, the maximum nanoparticle loading was selected as 1.0 g/L. The results achieved are much better than those of other studies carried out using different methods [21,22].

4.2. Effect of dye concentration on photodegradation efficiency

The effect of dye concentration on photodegradation efficiency was evaluated through conducting experiments using different concentrations of (20–100

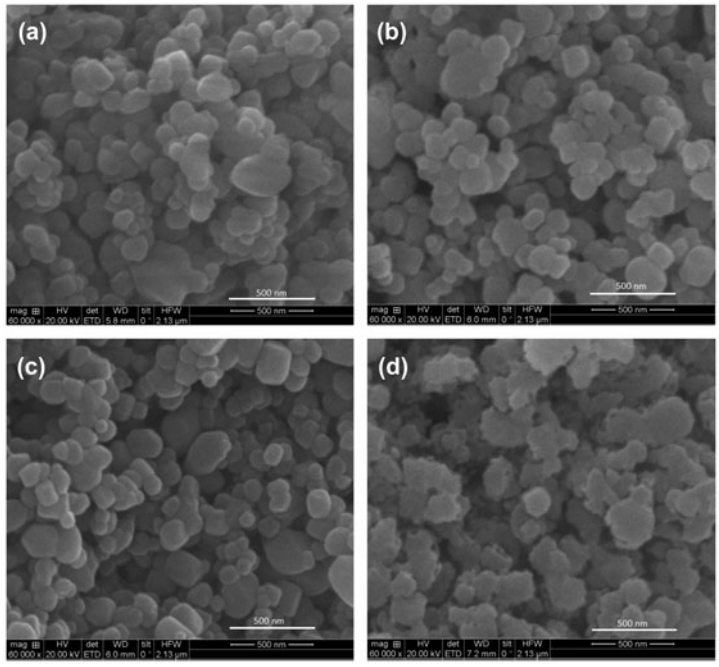

Fig. 3. SEM images of *in situ* surface-modified Fe:TiO_2 nanoparticles: (a) 1 mol % Fe_2O_3, 0.5 mL *n*-butylamine; (b) 1 mol % Fe_2O_3, 1.0 mL *n*-butylamine; (c) 2 mol % Fe_2O_3, 0.5 mL *n*-butylamine; and (d) 2 mol % Fe_2O_3, 1.0 mL *n*-butylamine.

mg/L) DO25. Fig. 5 shows that more the dye concentration, less the photodegradation efficiency. It can be attributed that increase in dye concentration interferes with light penetration; hence, the degradation efficiency will reduce—the effect similar to that observed in the case of pH.

Table 4
Characteristics of DO25

Characteristics	Identifications/properties
Name	DO25, Solvent Orange 105; 4-[N -(2-Cyanoethyl)-N-ethylamino]-4′
Synonyms	Nitroazobenzene; 3-[Ethyl [4-[(4-nitrophenyl)azo]phenyl] amino]-propanenitrile
Molecular formula	$C_{17}H_{17}N_5O_2$
Molecular weight	323.35
CAS registry number	31482-56-1 (12223-22-2)
Density	1.19
Melting point	155–160 ℃ (subl.)
Structure	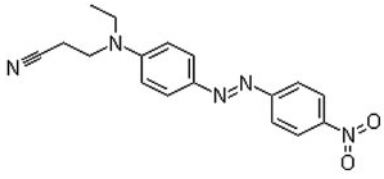

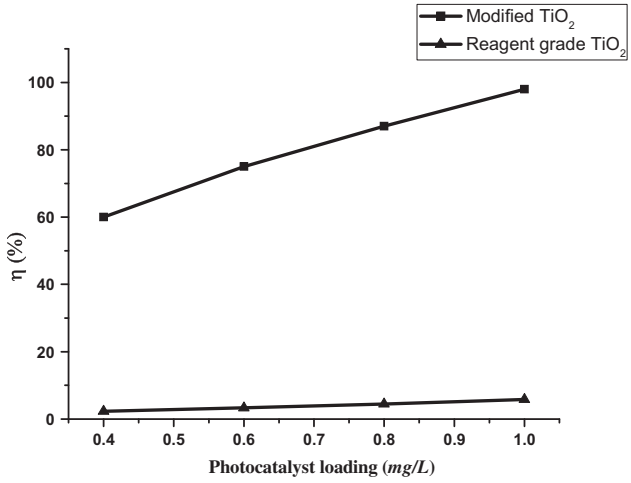

Fig. 4. Effect of photocatalyst loading on photodegradation efficiency of DO25 ($t = 2$ h).

4.3. Effect of pH on photodegradation of DO25

The amphoteric behavior of most semiconductor oxides influences the surface charge of the photocatalyst and the acid-base property of the metal oxide surfaces, which can make considerable implications upon their photocatalytic activity. In further

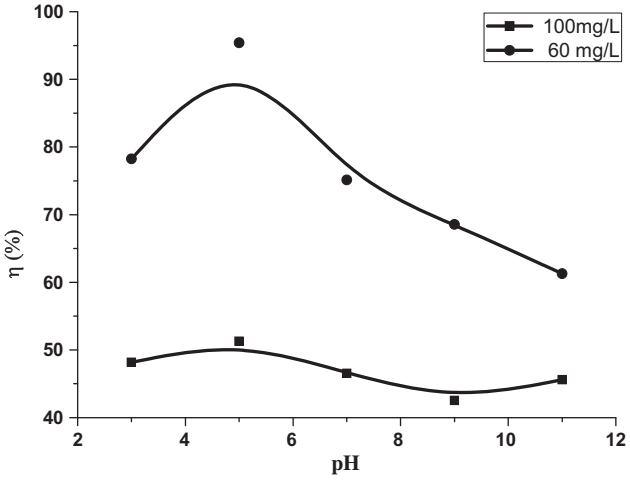

Fig. 5. Characteristic effect of pH on photodegradation of DO25 at different concentrations (60 and 100 mg/L) using *in situ* surface-modified iron-doped TiO_2 nanoparticles.

experiments, dye decolorizations were performed at various pH ranges (3–11) using 1.0 g/L of surface-modified Fe:TiO_2 nanoparticles for 2 h. The pH was adjusted using varying concentrations of 0.2 N HCl or NH_3OH. Fig. 6 illustrates the effect of pH. The maximum efficiency was observed at pH 5. As Fig. 6 indicates, effect of pH was more sensible for lower dye concentration. It reveals that changing pH is effective at lower concentration because when the dye concentration increases; it baffles light penetration and, as a result the photodegradation efficiency would reduce. The effect of pH can be explained based on

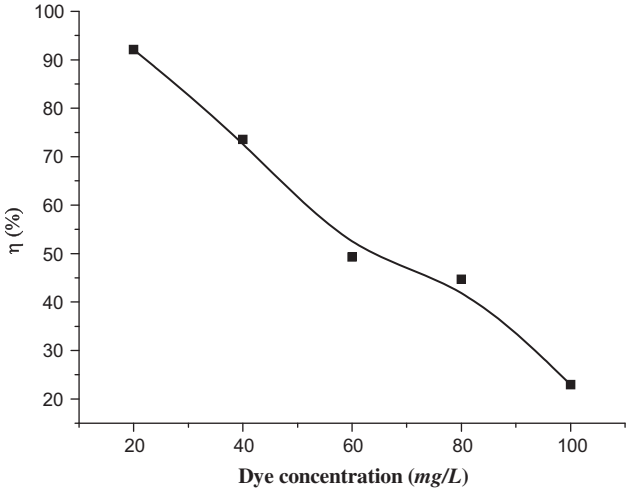

Fig. 6. Effect of dye concentration on photodegradation efficiency of DO25 using 1.0 g/L *in situ* surface-modified iron-doped TiO_2 nanoparticles for 2 h.

the zero point charge of TiO_2 nanoparticles. It is noteworthy that zero point charge (pzc) of reagent grade TiO_2 is between 5.6 and 6.4 [23], while pzc for modified Fe:TiO_2 nanoparticles was about 4.8 (the zeta potential analysis has not been presented here). It means, surface-modified Fe:TiO_2 nanoparticles are positively charged in acidic media (pH < 4.8), whereas they are negatively charged under neutral and alkaline condition (pH > 4.8) [24].

$$Ti^{IV} - OH + H^+ \rightarrow Ti^{IV} - OH_2^+ \quad (2)$$

$$Ti^{IV} - OH + OH^- \rightarrow Ti^{IV} - O^- + H_2O \quad (3)$$

The change in the pH of the solution varies with the dissociation of the dye molecule and the surface properties of the nanoparticles used. The initial adsorption of the dye molecules onto the nanoparticles greatly depends on the solution pH [24]. Increase in the degradation efficiency under the alkaline condition could be attributed to the increase in hydroxyl ions, which induce more hydroxyl radical formation.

4.4. Effect of type of nanoparticles on photodegradation of DO25

As mentioned earlier, *in situ* surface-modified Fe:TiO_2 nanoparticles were synthesized under four different conditions including dopant percentage and amount of surface modifier. The experiment was carried out under following conditions: nanoparticles loading 1.0 g/L; time duration 2 h; pH 5; and dye concentration 100 mg/L. Fig. 7 shows the effect of different types of nanoparticles synthesized on photodegradation efficiency. As Fig. 7 indicates, the maximum removal efficiency was achieved using Fe:TiO_2 II, i.e. 1 mol % dopant and 1.0 mL *n*-butylamine as surface modifier. Therefore, in comparing the effect of different parameters, Fe:TiO_2 II was used.

4.5. Mineralization of DO25

As irradiation time increases, dye molecules are degraded to components of lower molecular weight fractions, and consequently complete mineralization, which is observed from the chromatographs taken after each irradiation time. The complete mineralization is also confirmed from total organic carbon (TOC) analysis. Fig. 8 shows the degradation of organic carbon content for DO25 using 1.0 g/L surface-modified Fe:TiO_2 nanoparticles. Moreover, this figure demonstrates the formation of inorganic ions as a

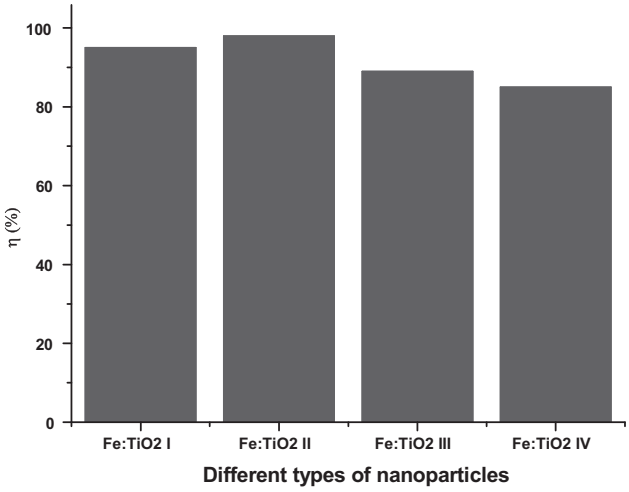

Fig. 7. Effect of type of nanoparticles on photodegradation of DO25 at pH 5 and dye concentration 80 mg/L using 1.0 g/L *in situ* surface-modified iron-doped TiO_2 nanoparticles. (I) 1.0 mol % dopant, 0.5 mL surface modifier; (II) 1.0 mol % dopant, 1.0 mL surface modifier; (III) 2.0 mol % dopant, 0.5 mL surface modifier; and (IV) 2.0 mol % dopant, 1.0 mL surface modifier.

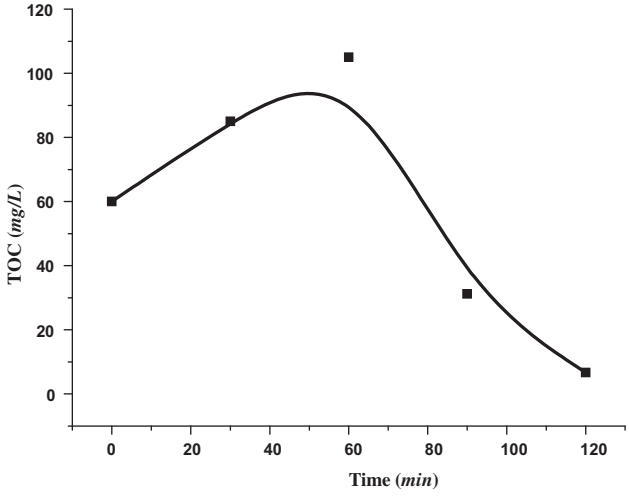

Fig. 8. Mineralization study of DO25 at pH 5 and dye concentration 100 mg/L using 1.0 g/L *in situ* surface-modified iron-doped TiO_2 nanoparticles.

function of time. As Fig. 8 indicates, there is an increase in TOC after 30 min, and again it decreases. This irregular increase may be due to *n*-butylamine used for surface modification of the Fe:TiO_2 nanoparticles; however, in the end, the dye was degraded significantly. This increase and subsequent decrease might be attributed to slight detachment of *n*-butylamine from the TiO_2 surface.

5. Conclusion

The *in situ* surface-modified iron-doped TiO_2 nanoparticles were successfully synthesized under mild hydrothermal conditions (p = autogeneous, $T = 100\,^{\circ}C$, $t = 16$ h). The characterization results revealed high crystallinity of nanoparticles. The photodegradation of DO25 under sunlight irradiation indicated significant efficiency of these nanoparticles compared with that of reagent grade TiO_2, which was negligible. Moreover, it was proved that dye solution was not only discolored but also mineralized. These results were achieved without supplying aeration and at limited dosage of nanoparticles (1.0 mg/L) to make the process more cost-effective. The nanoparticles synthesized can be used for tropical areas where free energy source, i.e. sunlight, is available.

Acknowledgment

The authors are grateful for the financial support provided by the Kurdistan University of Medical Sciences, Sanandaj, Kurdistan, Iran.

References

[1] H. Zollinger (Ed.), Color Chemistry: Synthesis, Properties and Applications of Organic Dyes and Pigments, 2nd ed., Wiley-VCH Verlag GmbH, Weinheim, 1991.
[2] A. Houas, H. Lachheb, M. Ksibi, E. Elaloui, C. Guillard, J.M. Hermann, Photocatalytic degradation pathway of Methylene Blue in water, Appl. Catal., B 31 (2001) 145–157.
[3] A.B. Prevot, C. Baiocchi, M.C. Brussino, E. Pramauro, P. Savarino, V. Augugliaro, G. Marcì, L. Palmisano, Photocatalytic degradation of acid blue 80 in aqueous solutions containing TiO_2 suspensions, Environ. Sci. Technol. 35 (2001) 971–976.
[4] V. Murugesan, S. Sakthivel, Photocatalytic degradation of leather dyes in aqueous solution using solar/UV illuminated TiO_2/ZnO, Proceedings of International Symposium on Environmental Pollution Control and Waste Management, 7–10 January 2002, Tunis (EPCOWM' 2002), pp.654–659.
[5] F. Sayilkan, M. Aailtürk, Ş. Şener, S. Erdemoğlu, M. Erdemoğlu, H. Sayilkan, Hydrothermal synthesis, characterization and photocatalytic activity of nanosized TiO_2 based catalysts for Rhodamine B degradation, Turk. J. Chem. 31 (2007) 211–221.
[6] C. Anderson, A.J. Bard, Improved photocatalytic activity and characterization of mixed TiO_2/SiO_2 and TiO_2/Al_2O_3, J. Phys. Chem. 101 (1997) 2611–2616.
[7] M.N. Rashed, A.A. El-Amin, Photocatalytic degradation of methyl orange in aqueous TiO_2 under different solar irradiation sources, Int. J. Phys. Sci. 2 (2007) 73–81.
[8] Y. Liu, J. Li, X. Qiu, C. Burda, Novel TiO_2 nanocatalysts for wastewater purification-tapping energy from the sun, Water Pract. Technol. 54 (2006) 47–54.

[9] B. Shahmoradi, I.A. Ibrahim, N. Sakamoto, S. Ananda, T.N.G. Row, K. Soga, K. Byrappa, S. Parsons, Y. Shimizu, In-situ surface modification of molybdenum doped TiO_2 organic-inorganic hybrid nanoparticles under hydrothermal conditions and treatment of pharmaceutical effluent, Environ. Technol. 31 (2010) 1213–1220.
[10] B. Shahmoradi, I.A. Ibrahim, N. Sakamoto, S. Ananda, R. Somoshekar, T.N.G. Row, K. Byrappa, Photocatalytic treatment of municipal wastewater using modified neodymium doped TiO_2 hybrid nanoparticles, Environ. Sci. Health. Part A 45 (2010) 1248–1255.
[11] B. Shahmoradi, K. Namratha, K. Byrappa, K. Soga, S. Ananda, R. Somashekar, Enhancement photocatalytic activity of modified ZnO nanoparticles with manganese additive, Chem. Res. Intermed. 37 (2011) 329–340.
[12] A.J. Maira, J.M. Coronado, V. Augugliaro, K.L. Yeung, J.C. Conesa, J. Soria, Fourier transform infrared study of the performance of nanostructured TiO_2 particles for the photocatalytic oxidation of gaseous toluene, J. Catal. 202 (2001) 413–420.
[13] C.C. Liu, Y.H. Hsieh, P.F. Lai, C.H. Li, C.L. Kao, Photodegradation treatment of azo dye wastewater by UV/TiO_2 process, Dyes Pigm. 68 (2006) 191–195.
[14] S.S. Lee, H.J. Kim, K.T. Jung, H.S. Kim, Y.G. Shul, Photocatalytic activity of metal ion (Fe or W) doped titania, Korean J. Chem. Eng. 18 (2001) 914–918.
[15] J. Li, L. Zheng, L. Li, Y. Xian, L. Jin, Fabrication of TiO_2/Ti electrode by laser-assisted anodic oxidation and its application on photoelectrocatalytic degradation of methylene blue, J. Hazard. Mater. 139 (2007) 72–78.
[16] S.L. Clescerl, A.E. Greenberg, A.D. Eaton, Standard Methods for Examination of Water and Wastewater, 21st ed., American Water Works Association, Washington, DC, 2005.
[17] C.J. Howard, T.M. Sabine, F. Dickson, Structural and thermal parameters for rutile and anatase, Acta Crystallogr. Sect. B 47 (1992) 462–468.
[18] N.S. Begum, H.M. Farveez, O.M. Hussain, Characterization and photocatalytic activity of boron-doped TiO_2 thin films prepared by liquid phase deposition technique, Bull. Mater. Sci. 31 (2008) 741–745.
[19] Q. Zhang, T.P. Chou, B. Russo, S.A. Jenekhe, G. Cao, Aggregation of ZnO nanocrystallites for high conversion efficiency in dye-sensitized solar cells, Angew. Chem. Int. Ed. 47 (2008) 2402–2406.
[20] D.L. Pavia, G.M. Lampman, G.S. Kriz, Infrared Spectroscopy, in: John Vondeling (Ed.), Introduction to Spectroscopy, 3rd ed., Brooks/Cole, Stamford, CT, 2001, pp. 13–101.
[21] A. Aleboyeh, H. Aleboyeh, Y. Moussa, Critical effect of hydrogen peroxide in photochemical oxidative decolorization of dyes: Acid Orange 8, Acid Blue 74 and Methyl Orange, Dyes Pigm. 57 (2003) 67–75.
[22] A. Maleki, A.H. Mahvi, R. Ebrahimi, Y. Zandsalimi, Study of photochemical and sonochemical processes efficiency for degradation of dyes in aqueous solution, Korean J. Chem. Eng. 27 (2010) 1805–1810.
[23] D. Chen, A.K. Ray, Photodegradation kinetics of 4-nitrophenol in TiO_2 suspension, Water Res. 32 (1998) 3223–3234.
[24] L.S. Murov, Handbook of Photochemistry, Marcel Dekker, New York, NY, 1973.